Highlights on Spanish Astrophysics X, Proceedings of the XIII Scientific Meeting of the Spanish Astronomical Society held on July 16 – 20, 2018, in Salamanca, Spain. B. Montesinos, A. Asensio Ramos, F. Buitrago, R. Schödel, E. Villaver, S. Pérez-Hoyos, I. Ordóñez-Etxeberria (eds.), 2019

Are we missing massive red galaxies at z>3?

Belén Alcalde Pampliega[1], Pablo G. Pérez-González[1,2], Guillermo Barro[3] Helena Domínguez Sánchez[4] and M. Carmen Eliche-Moral[5]

[1] Departamento de Física de la Tierra y Astrofísica, Faultad de CC Físicas, Universidad Complutense de Madrid E-2840 Madrid, Spain
[2] Centro de Astrobiología (CAB, INTA-CSIC), Carretera de Ajalvir km 4, E-28850 Torrejón de Ardoz, Madrid, Spain
[3] Astronomy Department,Department of Physics, University of the Pacific, Stockton, CA 95211, USA.
[4] Department of Physics and Astronomy, University of Pennsylvania, Philadelphia, PA 19104, USA.
[5] Instituto de Astrofísica de Canarias, Calle Vía Láctea, s/n, E-38205, La Laguna, Tenerife, Spain.

Abstract

We present the detection of a sample of galaxies which are extremely faint in the optical and near-infrared but bright at mid-infrared wavelengths. This population of galaxies, missed by the deepest HST surveys such as CANDELS or Hubble Frontier Fields, are considerably bright in IRAC. The bulk of the sample (65%) is located in a 2σ region around the main sequence. Approximately 20% of the Balmer Break Galaxies (BBGs) are very dusty starbursts with strong mid-to-far infrared detections and extreme star formation rates. The remaining, 15%, are located more than 2σ below the main sequence and might be either regular star-forming galaxies or quiescent systems. Nearly one third of them are MIPS emitters, most probably revealing the presence of an obscured AGN co-existing with the intense star formation, as measured by Herchel. Only 2 sources are detected in X-rays and 3 at sub-millimiter or radio wavelengths. Our results point out that BBGs significantly contribute (35%) to the general population of massive red galaxies at z$= 4-6$ and that one of every ten massive $\log(M/M_\odot) > 11$ galaxies in the local Universe was assembled in the first 1.5 Gyr after the Big Bang.

1 Introduction

Understanding when the first massive galaxies appeared in the Universe is essential for models of galaxy evolution. While the ΛCDM paradigm predicts that most massive halos assembled at lower redhshifts, observational studies suggest that the most massive local galaxies

($\log(M/M_\odot) > 11$) formed early in the universe [6, 5, 2]. Recently, many surveys have identified a substantial population of massive galaxies at redshifts up to $z \sim 4$, when the universe was only 1.5 Gyr old [10, 1] some of them showing evidences of evolved stellar populations [8]. Characterizing the star formation activity and the number density of massive high redshift is particularly important to improve our picture of galaxy evolution and to constrain galaxy formation models. A major complication to address these questions is gathering a complete, robust and un-biased census of massive galaxies up to the highest redshifts possible. Most studies up to date are based in UV-selected samples, which are particularly sensitive to detect young and/or blue system but are strongly biased against red, dusty or evolved galaxies. Thus, rest-frame UV-selected samples at high-redshift are likely incomplete, missing massive red galaxies which could potentially be identified with observations at longer wavelengths.

2 Selection process

Our selection technique is based on two conditions. BBG candidates are required to be bright in the first two channels of IRAC, [3.6] and [4.5] ≤ 24.5 mag, and undetected (dropouts) in the HST/F160W (H$\gtrsim$27) publicly available catalogues published by the CANDELS and 3D-HST teams —[3], [7], Barro et al. 2018, in prep.—). We have used TFIT residual frames to search for potential H-band dropouts with bright IRAC magnitudes. Briefly, TFIT is used to generate a model of the IRAC image by convolving the high spatial resolution HST/F160W mosaic with the appropriate PSF transformation kernel. Then, the fluxes on the resulting "template" image are scaled to those of the galaxies in the IRAC frame on a galaxy-by-galaxy basis. Lastly, TFIT subtracts the scaled "template" image from the original IRAC mosaic creating a residual frame which is used to verify the quality of the source extraction and flux measurements. Before searching for BBG candidates in the residual IRAC image, we applied three different cleaning masks for the bright H-band sources, brightest stars and artifacts. We also applied a mathematical morphology method to the regions around H-band bright sources to avoid extra flux arising from their wings.

3 Observed IR colors, photometric redshifts and masses of BBGs

In this Section we analyze the distribution of observed colors, photometric redshifts and stellar mass of the 33 BBGs using the results from the UV-to-FIR SED fitting techniques. We also compare BBGs with two samples constructed with the CANDELS GOODS H-band selected catalogs. The mass-selected sample is composed by massive ($M > 10^{10}\,M_\odot$) galaxies at $z > 3$. The color-selected sample, aimed to reproduce our BBG selection, is composed by red ($H - [3.6] > 2.5$) faint ($H > 25$) galaxies.

The $H - [3.6]$ red colors of most of our sources are compatible with evolved populations or heavily extincted starbursts. However, our sample includes a distinct population of blue (both in their observed $H - [3.6]$ and their UVJ rest-frame colors) galaxies. This population have similar SEDs to galaxies from the mass-selected sample. They indeed present uncommon

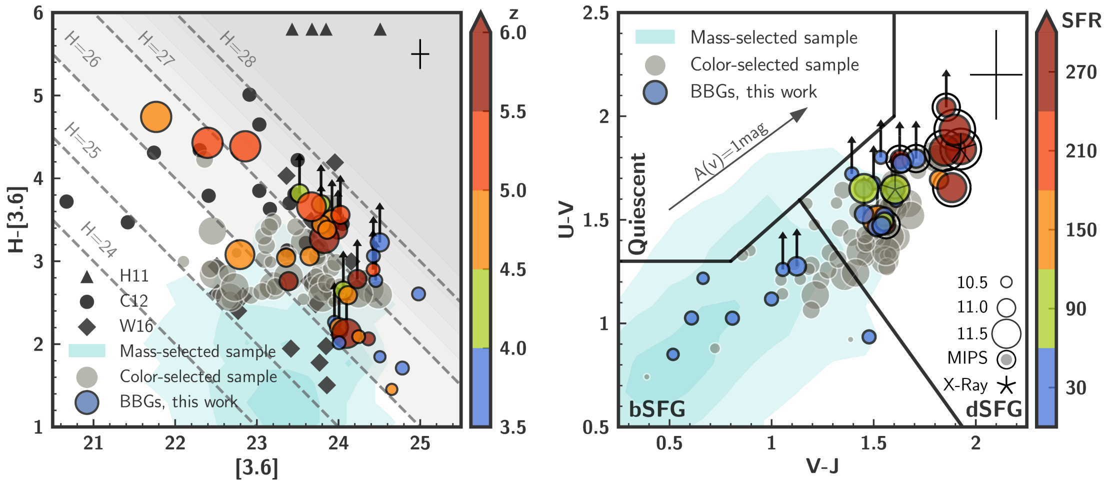

Figure 1: *Left panel:* Observed-frame $H-[3.6]$ color plotted versus the observed [3.6] magnitude for our sample of BBGs, color-coded by their photometric redshift and scaled in size as a function of their stellar mass (legend shown in right panel). *Right panel:* Rest-frame $U-V$ vs. $V-J$ color-color plot, where BBGs are color-coded by SFR and scaled by stellar mass.

blue [3.6]-[4.5] colors that might be caused by the presence of an emission line in the [3.6] band (converting them in red sources in our selection color $H-[3.6]$). We also note that they correspond to some of the less massive ($\mathrm{M} < 10^{10.5}\mathrm{M}_{\odot}$) BBGs in our sample. Therefore, their detection might be a consequence of our improved photometric technique to recover faint sources and reliable upper limits. In addition, we compare our sample of BBGs with the samples of galaxies of similar nature presented in [4, 1], and [9] (see. left panel legend in Fig. 1).

Subdividing BBGs by their rest-frame UVJ colors (see right panel in Fig. 1), we find a mix of blue SFGs and dusty SFGs. Although no clearly quiescent galaxies are found, 3 of our BBGs (located close to the quiescent boundary) have mass-weighted ages that are large enough ($\mathrm{t}_m \geqslant 0.9$ Gyr) to be consistent with evolved or quiescent galaxies.

We have also proved that a $H-[3.6]$ color and IRAC magnitude cuts imply a redshift selection as shown in the the left panel of Fig. 2. The redshift distributions, of both the BBGs and the color-selected sample peak at $z = 4-5$, while the mass-selected sample presents an exponentially decreasing redshift distribution (typical of flux limited samples). Our selection criterion is also adequate to probe the high mass end of the stellar mass function ($\mathrm{M} \gtrsim 10^{10}\mathrm{M}_{\odot}$). The BBG stellar mass distribution peaks at $\mathrm{M} \sim 10^{10.5}\mathrm{M}_{\odot}$. The color-selected sample presents a comparable histogram with a longer tail at higher masses due to their brighter IRAC magnitudes. The mass-selected sample, in contrast, presents a distribution that decreases with increasing masses.

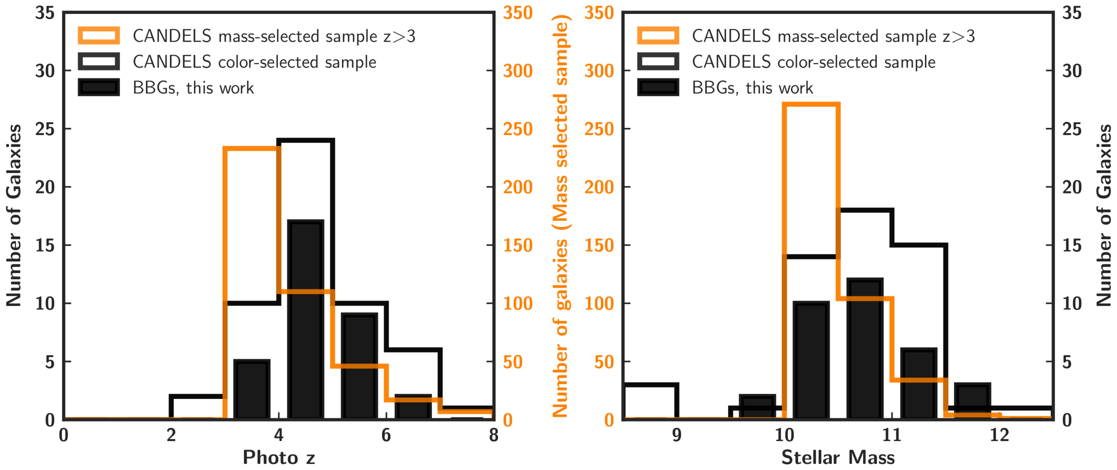

Figure 2: Photometric redshift (*left panel*) and stellar mass (*right panel*) distributions of our sample of BBGs compared to those of the color-selected and mass-selected CANDELS samples. Given the substantially higher number of galaxies among the mass-selected sample, a different axis has been used for it, as indicated by the orange labels.

4 BBGs and the star formation main sequence

From the SED modelling, we find a strong evidence that massive red galaxies at $z = 3 - 6$ span a diverse range in stellar population properties. In order to understand the nature of the heterogeneous sample of BBGs, we have divided the sources in three star formation regimes according their position with respect to the main sequence (MS) from GOODS: starbursts, MS and sub-MS galaxies (Fig. 3). Analyzing the average SEDs of BBGs, we confirm that, in general, mass-selected galaxies present bluer SEDs than those from the BBG and the color-selected samples. However we identify a subsample of BBGs in the MS which are blue and harder to separate from the general population probed by a mass-selected sample. In addition, we find a small number of sub-MS galaxies (16%), most of them with $\mathrm{M} < 10^{10.5}\mathrm{M}_{\odot}$, characterized by low extinctions and larger mass-weighted ages (t_m). On the other hand, starbursts are found in the most massive ($\mathrm{M} > 10^{10.5}\mathrm{M}_{\odot}$) galaxies from the BBGs (20% of the total number of BBGs are starburst) and color-selected (15%) sources. Starbursts are characterized by very high extinctions and young t_m. It is remarkable that 5 BBGs out of the 6 starbursts have FIR emission, all are at least detected at 24μm, 3 emit at submillimeter wavelengths and one is an X-Ray source as well. This suggests that a significant fraction of the BBGs ($\sim$25 and up to $\sim$75%) might host an obscured AGN. MS galaxies represent a constant proportion of BBGs ($\sim$65%) and color-selected ($\sim$60%) up to the highest masses $\mathrm{M} \sim 10^{11.5}\mathrm{M}_{\odot}$. However, an important fraction (25%) of the MS galaxies have been assigned with a SFR lower limit (given their detection by MIPS, but their high redshift (z> 5) prevents from obtaining a robust SFR estimation) and may correspond to starburst galaxies. BBGs in the MS present a larger scatter in their extinctions, mass-weighted ages and and UVJ colors.

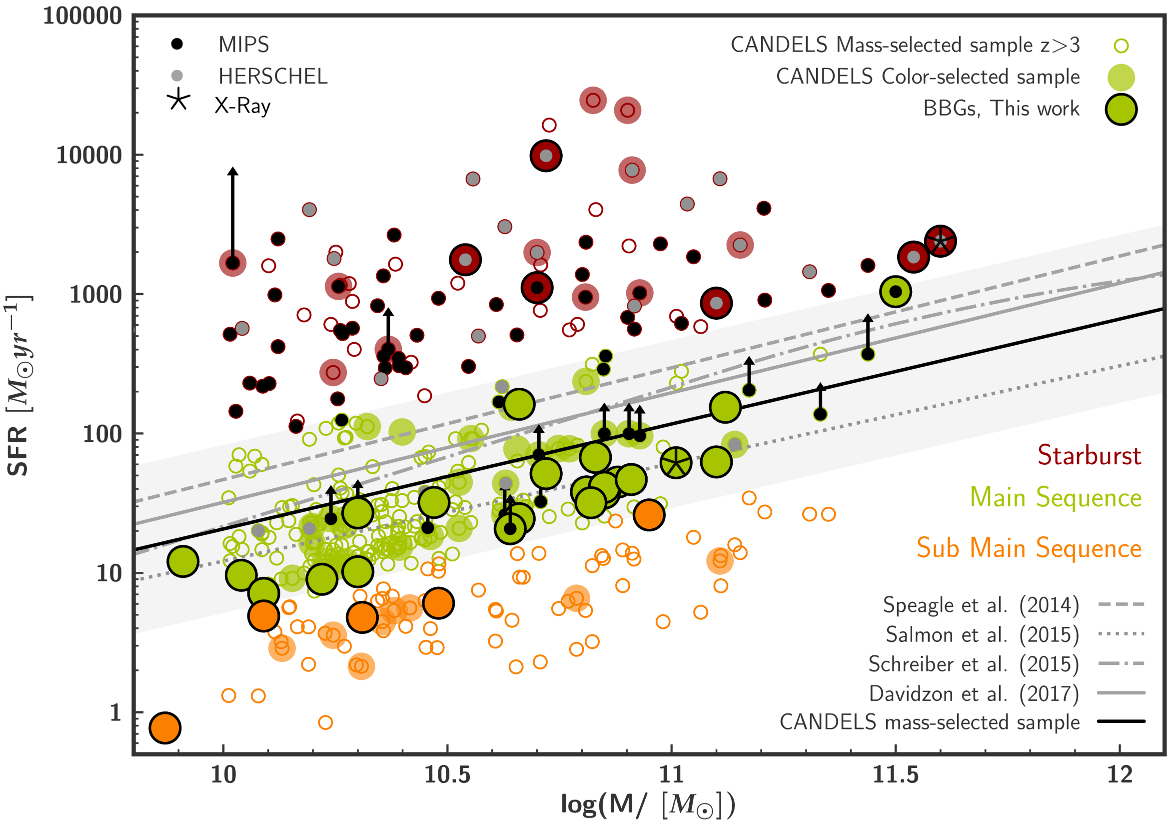

Figure 3: SFR vs stellar mass plane for the CANDELS comparison samples (color-selected —filled symbols— and mass-selected —open symbols—) and the BBGs (filled symbols enclosed by a black circle) reported in this work, color coded according to their position with respect to the main sequence: starburst, MS and sub-MS galaxies are shown in deep-red, green, and orange respectively. The MS from the literature at $z = 4$ are shown with different grey lines (see the legend in the panel). The MS inferred for the CANDELS mass-selected sample is shown with a black solid line. The grey-shaded region delimits the 2σ area around the MS. MIR/FIR emitters are marked with an enclosed black/grey circle. The galaxies with MIPS detections but no IR-derived SFRs are shown as lower limits. X-rays emitters are also highlighted with a star symbol.

5 The role of BBGs in galaxy evolution

We have found that the red BBGs presented in this work account for 7% of the total number density of $\log(\mathrm{M}/\mathrm{M}_\odot) > 10$ galaxies at $z > 3$ found by public catalogues such as CANDELS' or 3D-HST's. Our BBGs are, however, a major contributor (30%) to the general (adding catalogue galaxies and our BBGs) population of $\log(\mathrm{M}/\mathrm{M}_\odot) > 11$ galaxies at $4 < z < 6$ and, more remarkably, to the population of red massive galaxies (i.e., evolved or dusty systems) in the same redshift interval, accounting for 35% of this population. Adding the BBGs presented in this work to the known population of $4 < z < 6$ and $\mathrm{M} > 10^{11}\,\mathrm{M}_\odot$ we have found a total number density of $1.1{\times}10^{-5}$galaxies/Mpc^3. This represents 8% of the the number density of local M$> 10^{11}\,\mathrm{M}_\odot$ meaning that nearly 1 in 10 massive galaxies in the local Universe must have assembled more than $10^{11}\,\mathrm{M}_\odot$ in the first 1.5 Gyr of the Universe.

6 Summary and conclusions

Combining ultra-deep data taken in the WFC3 $F160W$ and IRAC 3.6 and 4.5 μm bands, we have identified a sample of 33 IRAC bright/optically faint Balmer Break Galaxies (BBGs) at high redshift within the two GOODS fields. We have also proved the effectiveness of a $H - [3.6]$ color and IRAC magnitude cuts in selecting red massive galaxies at $z > 3$.

Most of our sources are compatible with heavily extincted starbursts and 30% of them being compatible with evolved populations. This population of BBGs is major contributor (30%) to the general (adding catalogued galaxies and our BBGs) population of $\log(\mathrm{M}/\mathrm{M}_\odot) >$ 11 galaxies at $4 < z < 6$ and, more remarkably (35%), to the population of red massive galaxies in the same redshift interval.

Accounting for this kind of objects is key to understand the population of massive galaxies at high redshift and their number density is specially important among red massive galaxies at $z = 4 - 6$. Moreover, BBGs represents 8% of the the number density of local M$> 10^{11}\,\mathrm{M}_\odot$ meaning that nearly 1 in 10 massive galaxies in the local Universe must have assembled more than $10^{11}\,\mathrm{M}_\odot$ in the first 1.5 Gyr of the Universe.

Acknowledgments

We acknowledge support from the Spanish Programa Nacional de Astronomía y Astrofísica under grants AYA2015-63650-Pand BES-2013-065772. We also acknowledge SEA support for young astronomers.

References

[1] Caputi,K., Dunlop, J.S., McLure, R.J., 2011, ApJ, 750(1):L20x

[2] Grazian,A., Fontana, A, Santini, P. 2015 575:A96

[3] Guo, Y., Ferguson, H. C, Giavalisco, M. 2013, apjs, 207:24

[4] Huang,J-S, XZ Zheng, Rigopoulou,D. 2011, Apjs, 742(1):L13

[5] Mancini, C., Matute, I., Cimatti, A., 2009, A&A, 500(2):705–723

[6] Pérez-González, P. G., Rieke, G. H., Villar,V.,2008, ApJ, 675(1):234

[7] Skelton,R. E., Whitaker,K. E., Momcheva,I. G. 2014, apjs, 214:24

[8] Straatman,C. M. S., Spitler,L. R., Quadri,R. F. 2016, apj, 830:51

[9] Wang,T., Elbaz,D. , Schreiber,C. 2016, apj, 816:84

[10] Wiklind,T., Dickinson,M., Ferguson,H. C., 2008, apj, 676:781–806